Electronic Properties of Mixed Valence Manganates: the Role of the Cationic Vacancies

T. Boix, F. Sapiña,* Z. El-Fadli,† E. Martinez, and A. Beltrán

Institut de Ciència dels Materials de la Universitat de València, C/Doctor Moliner 50, E−46100 Burjassot, Spain

J. Vergara and R. J. Ortega

Departamento de Física, Universidad Pública de Navarra, E−31006 Pamplona, Spain

K. V. Rao

Department of Condensed Matter Physics, The Royal Institution of Technology, S-10044 Stockholm, Sweden

Received November 14, 1997. Revised Manuscript Received March 11, 1998

Single-phase perovskites in the solid solution series $La_{1-x}Na_xMnO_{3+\delta}$ have been obtained using a soft treatment, which makes possible strict stoichiometric control. Under these conditions, it becomes possible to systematically study the influence of the sodium content on the electronic properties of materials in this series. As long as all the samples have practically the same Mn^{4+} content (33%), the number of vacancies at A and B sites of the perovskite structure depends on the sodium content, and it decreases as x increases. Susceptibility to alternating current, magnetization, resistivity, and magnetoresistivity measurements have allowed us to establish relevant points of the electronic phase diagram of this alkali-metal-doped lanthanide manganate system. These results, together with those previously obtained for $La_{1-x}K_xMnO_{3+\delta}$, reveal the existence of a correlation between the critical temperature for ferromagnetic ordering and the concentration of vacancies at the B sites, v_B, in samples with a fixed concentration of Mn^{4+}. Such a correlation can be understood in terms of a magnetic phase segregation model in which the materials are thought of as composed by clusters, formed by the vacancies (trapping centers for mobile holes) and neighboring Mn cations (on which holes are trapped), and a matrix, formed by the remaining Mn cations. Within this model, the decrease in the number of mobile holes in the matrix is the cause of the decrease in the critical temperature with v_B.

Introduction

The well-known interest for technological applications of alkaline-earth-doped lanthanide manganates, $Ln_{1-x}A_xMnO_{3\pm\delta}$ (Ln = La, Pr, Nd, Sm; A = Ca, Sr, Ba, Pb), has been revived after the recent discovery of colossal magnetoresistance (CMR) in these materials.[1]

To tailor the physical properties of these materials for applications, as well as to understand the basic aspects of the interaction mechanism between the manganese ions, systematic explorations of mixed-valence alkaline-earth lanthanide manganates have been performed.[2] These studies show the importance of the mean oxidation state of manganese ions, having its optimum value close to 3.33. A relationship between the transition temperatures and the mean size of cations at the A sites, $\langle r_A \rangle$, has been observed for samples with such a concentration of Mn^{4+}.[3] The $\langle r_A \rangle$ value determines in practice the structural distortion of the perovskite structure, that is, the Mn−O−Mn angle and, hence, the transfer integral t_σ^F between Mn^{3+} and Mn^{4+} ions.

Despite the above, from the results of the study on the $La_{1-x}K_xMnO_{3+\delta}$ system,[4] we recently concluded that the values of the Mn^{4+} concentration, c, and the mean size of the cations at the A sites, $\langle r_A \rangle$, were not able to characterize by themselves the electronic behavior of these materials. Then, we proposed the use of a new parameter in order to fully characterize these compounds. According to our results, this additional pa-

* Corresponding author. E-mail: fernando.sapina@uv.es. Fax: 34-6-3864858. Phone: 34-6-3983150.

† On leave from the Département de Chimie, Faculté des Sciences, Université Abdelmalek Essaadi, Tétouan, Maroc.

(1) (a) Kusters, R. M.; Singleton, J.; Keen, D. A.; McGreevy, R.; Hayes, W.; *Phys. B* **1989**, *155*, 362. (b) von Helmot, R.; Wecker, J.; Holzapfel, B.; Schultz, L.; Samwer, K. *Phys Rev. Lett.* **1993**, *71*, 2331. (c) Jin, S.; Tiefel, T. H.; McCormack, M.; Fastnacht, R. A.; Ramesh, R. L.; Chen, H. *Science* **1994**, *64*, 413.

(2) (a) Schiffer, P.; Ramirez, A. P. Bao, W.; Cheong, S. W. *Phys. Rev. Lett.* **1995**, *75*, 3336. (b) Urushibara, A.; Moritomo, Y.; Arima, T.; Asamitsu, A.; Kido, G.; Tokura, Y. *Phys. Rev. B* **1995**, *51*, 14103.

(3) (a) Maignan, A.; Caignert, V.; Simon, Ch.; Hervieu, M.; Raveau, B. *J. Mater. Chem.* **1995**, *5*, 1091. (b) Hwang, H. Y.; Cheong, S. W.; Radaelli, P. G.; Marezio, M.; Batlogg, B. *Phys. Rev. Lett.* **1995**, *75*, 914. (c) Mahesh, R.; Mahendiran, R.; Raychaudhuri, A. K.; Rao, C. N. R. *J. Solid State Chem.* **1995**, *120*, 204.

(4) Ng-Lee, Y., Sapiña, F.; Martinez-Tamayo, E.; Folgado, J. V.; Ibañez, R.; Beltrán, D.; Lloret, F.; Segura, A. *J. Mater. Chem.* **1997**, *7*, 1905.

S0897-4756(97)00749-7 CCC: $15.00
Published on Web 05/05/1998

rameter could be the concentration of vacancies at the B perovskite sites, v_B.

To progress in the understanding of the basic aspects involved in CMR, we have approached the systematic study of the $La_{1-x}Na_xMnO_{3+\delta}$ series. Careful control of the synthetic variables has allowed us to determine relevant points in the electronic phase diagram of this system. The present results, together with those previously obtained in the case of the $La_{1-x}K_xMnO_{3+\delta}$ system, clearly show the existence of a correlation between the critical temperature for ferromagnetic ordering and the concentration of vacancies at the B sites, v_B, in samples with a fixed concentration of Mn^{4+} (close to the optimal).

Experimental Section

Aqueous solutions of metal acetates with molar nominal compositions La:Na:Mn = 1 − *x*:*x*:1.00, with *x* = 0.00, 0.03, 0.06, 0.09, 0.12, and 0.15, were prepared as follows. $NaHCO_3$ was dissolved in 100 mL of glacial acetic acid. The addition of La_2O_3 led to a suspension, which was gently heated while stirring for 15 min. After addition of 20 mL of H_2O, a transparent solution resulted. After cooling, $Mn(CH_3COO)_2 \cdot 4H_2O$ was added and dissolved upon stirring. The masses of the different reagents were adjusted to give 5 g of perovskite. Droplets of the resulting pink pale acetic acid solutions were flash frozen by projection on liquid nitrogen and, then, freeze-dried at a pressure of 10^{-2} atm. In this way, dried solid precursors were obtained as pink loose powders.

Preliminary experiences show that the minimum temperature at which the perovskite phase is obtainable is 700 °C (12 h) for all compositions investigated in this work and was thus adopted for thermal treatment of the perovskite precursors. After cooling of the furnace, the samples were ground, pelletized, and heated under oxygen flow at 1000 °C for 48 h. The resulting pellets were then annealed at 750 °C for 70 h.

Lanthanum, sodium, and manganese contents were determined by atomic absorption using a Perkin-Elmer 300 AA spectrophotometer. The mean oxidation state of manganese ions and, thus, the oxygen content, was determined by redox back-titration of Fe(II) with potassium dichromate in HCl using a Crison CompacT titrator.

Powder diffraction patterns were obtained using a Siemens D501 diffractometer, using secondary graphite-monochromated Cu Kα radiation. To reduce preferred orientation, the samples were dusted through a sieve on the holder surface. All X-ray data analyses were performed using the FULLPROF program.[5]

Magnetic susceptibility measurements were performed in a homemade ac susceptometer, in the temperature range 80−345 K, at magnetic field amplitudes 1 and 10 Oe. The working frequency was 181 Hz.

Magnetization measurements were performed in a Quantum Design SQUID magnetometer, in the temperature range 10−340 K, at magnetic fields up to 10 kOe.

Resistivity and magnetoresistance measurements were made by both the standard DC four probe technique and by using AC-resistance bridge (working at 75 Hz) from ASL, in the temperature tange 77−340 K, at fields up to 10 kOe. It is informative to point out that the results were identical from the two methods, for a given sample.

Results

Chemical Characterization. Table 1 summarizes the results of the chemical analyses. As can be observed, the actual sodium content of all the samples is practically equal to the nominal one. On the other hand, the oxygen content has been determined from the analitically calculated value of the mean oxidation state of the manganese ions and metal contents (Table 1). The manganese mean oxidation state is practically constant, being 3.33 ± 0.02. The effect of the increase in the sodium content is a decrease of the oxygen excess (for *x* = 0.00, $\delta = 0.17$; for *x* = 0.15, $\delta = 0.01$). Stoichiometries in Table 1 reflect previous results based on neutron diffraction, and high-resolution transmission electron microscopy experiences[6] that show that the uptake of extra oxygen in $La_{1-x}A_xMnO_{3+\delta}$ is accommodated by vacancies at the A and B perovskite sites, a result that also is consistent with density measurements.[7]

Table 1. Chemical Analysis for Samples of Nominal Composition $La_{1-x}Na_xMnO_{3+\delta}$[a]

x	La/Mn	Na/Mn	% Mn^{4+}	δ	stoichiometry
0.00	1.00	0.00	35	0.16	$La_{0.949}Mn_{0.949}O_3$
0.03	0.97	0.03	30	0.13	$La_{0.929}Na_{0.029}Mn_{0.958}O_3$
0.06	0.94	0.07	31	0.10	$La_{0.910}Na_{0.068}Mn_{0.968}O_3$
0.09	0.90	0.09	35	0.07	$La_{0.879}Na_{0.088}Mn_{0.977}O_3$
0.12	0.88	0.13	33	0.05	$La_{0.866}Na_{0.128}Mn_{0.984}O_3$
0.15	0.86	0.15	31	0.02	$La_{0.854}Na_{0.149}Mn_{0.993}O_3$

[a] $La_{1-x}Na_xMnO_{3+\delta}$ nomeclature is used for the sake of simplicity. The correct notation, from the structural point of view, is shown in the last column.

Structural Characterization. X-ray powder diffraction patterns shown in Figure 1 for $La_{1-x}Na_xMnO_{3+\delta}$ ($0 \le x \le 0.15$) were completely indexed in the rhombohedral perovskite-type structure. The structures of the perovskite phases have been refined in space group *R*-3*c*, in the hexagonal setting, from room-temperature powder X-ray diffraction data. The starting structural model used[6] was that of the $La_{0.95}Mn_{0.95}O_3$. The fits were performed using pseudo-Voigt peak-shape function. In the final runs, usual profile parameters (scale factors, background coefficients, zero-points, half-width, pseudo-Voigt, and asymmetry parameters for the peak shape) and atomic positions were refined. Isotropic thermal parameters were set at 0.3 and 0.7 $Å^2$ for metals and oxygen atoms, respectively, and an overall thermal parameter was also refined. In the structural models, La and Na are considered to be disordered in A sites, and their occupancies were fixed to give the oxygen stoichiometry and metal contents obtained by chemical analysis. Refined structural parameters and residuals, R_p, R_{wp}, R_B, and R_F are listed in Table 2. R_p and R_{wp} are the conventional (background corrected) peak only Rietveld profile and weighted profiles residuals. R_B and R_F are the integrated intensity and structure factor residuals, respectively. In Table 3 a selected list of bond distances and angles, as well as cell parameters for rhombohedral setting, are summarized. Figure 2 shows the variation of the hexagonal cell volume with *x*. *V* monotonically decreases with *x*, a striking result taking into account the sizes of the Na^+ and La^{3+} cations only.

Magnetic Properties. We have measured hysteresis loops at 10 K, at applied magnetic fields up to 9 kOe, after cooling in zero magnetic field. The knee of magnetization is reached at 5 kOe, above which the

(5) Rodriguez-Carvajal, J. FULLPROF Program, personal communication.

(6) Van Roosmalen, J. A. M.; Cordfunke, E. H. P.; Helmholdt, R. B.; Zandbergen, H. W. J. *Solid State Chem.* **1994**, *110*, 100.
(7) Van Roosmalen, J. A. M.; Cordfunke, E. H. P. *J. Solid State Chem.* **1994**, *110*, 106.

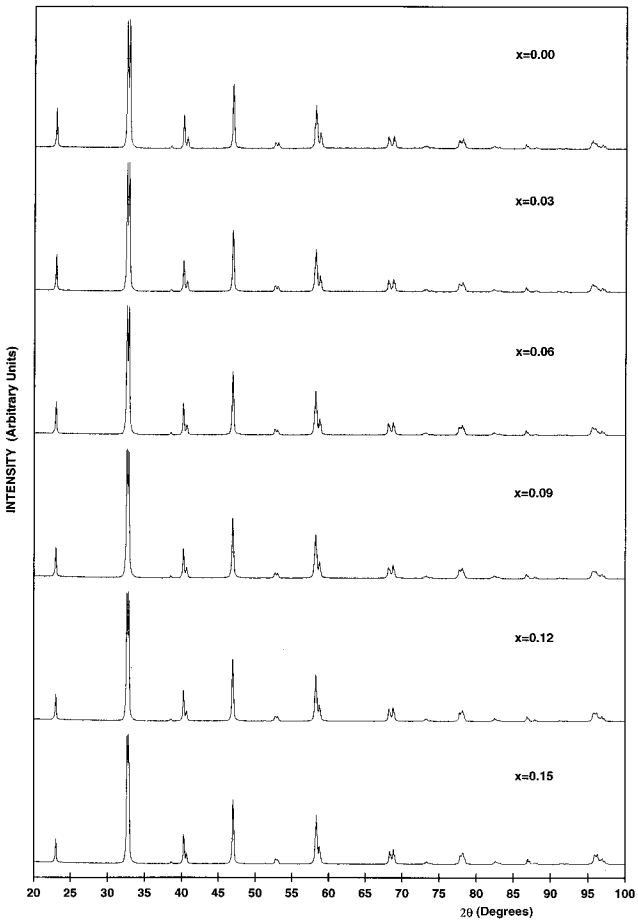

Figure 1. X-ray powder diffraction patterns of $La_{1-x}Na_xMnO_{3+\delta}$.

magnetization changes linearly with the field. A linear extrapolation at $H = 0$ has enabled us to derive the spontaneous magnetization, M_S(10 K). In all samples except $x = 0.00$, the observed spontaneous magnetizations are very close to the theoretical spontaneous magnetization, M_S^{cal}, calculated considering the actual mixed valence of Mn ions in these compounds. The reduced spontaneous magnetization observed in the case of the $x = 0.00$ material suggests that it has a canted ferromagnetic structure. Notwithstanding, the canting effect could not explain by itself the reduction of the magnetic moment observed by magnetization.[13a] We will return to this subject later on. On the other hand, the behavior of the sample $x = 0.03$ is within the limiting range between the canted (noncollinear) and the pure ferromagnetic arrangement of the spin layers.[13] These results are summarized in Table 4.

The temperature dependence of the magnetization was measured at a field of 10 Oe during warming runs, at temperatures ranging between 10 and 340 K. The samples were first cooled in such applied field. The curves are represented in Figure 3a for the whole series of samples. The magnetization decreases with the increase in temperature and presents an abrupt drop, corresponding to the transition from ferromagnetic to paramagnetic states. Estimated transition temperatures, T_M, are given in Table 4.

The ferromagnetic phase transition temperatures for all samples were validated by measuring the thermal dependence of both the in-phase, χ', and the out-of-phase, χ'', components of the ac magnetic susceptibility, at temperatures in the range 80−340 K. Parts a and b of Figure 4 show the thermal variation of the in-phase component of the ac susceptibility for samples $x = 0.03$ and 0.06. The χ' curves show an abrupt break at T_c as the temperature is lowered, which coincides with the appearance of an out-of-phase signal in the χ'' curves. This behavior clearly indicates that the system undergoes a phase transition from a paramagnetic to a long-range ordered magnetic state with a ferromagnetic component. The T_c results are shown in Table 4. Upon further cooling, both χ' and χ'' reach a maximum, and then decrease, presumably due to magnetic anisotropy.

Transport and Magnetotransport Properties. Figure 3b shows the temperature dependence of the resistivity at zero field for the whole series of samples. As the temperature is lowered, all samples except $x = 0.00$ exhibit a change in electrical properties, from insulator to metallic-like behavior. Thus, a maximum in each curve of resistivity versus temperature, characteristic of the semiconductor-to-metal transition, is observed at a temperature, T_R, close to that at which spontaneous magnetization appears. T_R values are listed in Table 4. The sample $x = 0.00$ exhibits a semiconductor-like temperature-dependent resistivity in the whole range of temperatures available in our experiments. The application of a magnetic field reduces significantly the resistivity below the transition temperatures. In parts a and b of Figure 4 the thermal variation of the magnetoresistance, defined as $-(\rho(T,H) - \rho(T,0))/\rho(T,0)$, has been represented for the samples $x = 0.03$ and 0.06, respectively, as representatives of the observed behavior. Upon cooling, a peak or an inflection in the magnetoresistance is observed at temperatures T_{MR} (see Table 4), very close to the paramagnetic insulator−ferromagnetic metal transition in all cases. At lower temperatures, the magnetoresistance increases monotonically.

From both magnetic and electrical behaviors, we can summarize the electronic phase diagram of the system $La_{1-x}Na_xMnO_{3+\delta}$ as represented in Figure 5. Data corresponding to $La_{1-x}K_xMnO_{3+\delta}$ have been included for comparison. Several electronic phases are observed. At low temperature, samples are ferromagnetic metals (FM) for $x \geq 0.06$, whereas the sample $x = 0.00$ is a noncollinear ferromagnetic insulator (NCFI). The sample $x = 0.03$ exhibits a behavior in the limiting range between FM and NCFI. At high temperatures, all the samples behave as paramagnetic insulators (PMI). The transition temperature increases with x, reaching its maximum value, 330 K, at $x = 0.15$.

(8) (a) Voorhoeve, R. J. H.; Remeika, J. P.; Trimble, L. E.; Cooper, A. S.; Disalvo, F. J.; Gallagher, P. K. *J. Solid State Chem.* **1975**, *14*, 395. (b) Shimura, T.; Hayshi, T.; Inaguma, Y.; Itoh, M. *J. Solid State Chem.* **1996**, *124*, 250.
(9) Shannon, R. D. *Acta Crystallogr.* **1976**, *A32*, 751.
(10) García-Muñoz, J. L.; Suaaidi, M.; Fontcuberta, J.; Rodriguez-Carvajal, J. *Phys. Rev. B* **1997**, *55*, 34.
(11) Ibarra, M. R.; Algarabel, P. A.; Marquina, C.; Blasco, J.; García, J. *Phys. Rev. Lett.* **1995**, *75*, 3541.
(12) De Gennes, P. G. *Phys. Rev.* **1960**, *116*, 141.
(13) (a) Alonso, J. A.; Martinez-Lope, M. J.; Casais, M. T.; Muñoz, A. *Solid State Commun.* **1997**, *102*, 7. (b) Wollan, E. O.; Koehler, W. C. *Phys. Rev.* **1955**, *100*, 545. (c) Goodenough, J. B. *Phys. Rev.* **1955**, *100*, 564.

Table 2. Structural Data for the X-ray Powder Diffraction Studies of $La_{1-x}Na_xMnO_{3+\delta}$[a]

x	0.00	0.03	0.06	0.09	0.12	0.15
a	5.5168(5)	5.5138(5)	5.5105(5)	5.5057(4)	5.4996(4)	5.4928(4)
c	13.3337(6)	13.3338(6)	13.3344(6)	13.3326(5)	13.3317(5)	13.3273(5)
x_0	−0.5485(13)	−0.5501(11)	−0.5475(12)	−0.5489(11)	−0.5459(11)	−0.5461(11)
R_p	11.0	9.7	9.3	8.9	8.5	8.3
R_{wp}	13.2	12.5	12.2	11.5	12.3	12.0
R_B	3.00	3.15	2.74	2.59	3.20	2.40
R_F	3.33	4.09	2.95	2.99	4.35	2.63

[a] Space group: *R*-3*c*, hexagonal setting. La, K (6a), (0, 0, 1/4); Mn (6b), (0, 0, 0); O (18e), (x, 0, 1/4).

Table 3. Selected Bond Distances (Å) and Angles (deg) and Cell Parameters and Volume for the Rhombohedral Cells of $La_{1-x}Na_xMnO_{3+\delta}$

x	0.00	0.03	0.06	0.09	0.12	0.15
Mn−O	1.960(4) (×6)	1.961(3) (×6)	1.959(3) (×6)	1.958(4) (×6)	1.954(3) (×6)	1.953(3) (×6)
Mn−O−Mn	164.3(3)	163.8(3)	164.6(3)	164.2(2)	165.2(3)	165.1(3)
La−O	2.747(3) (×6)	2.747(2) (×6)	2.746(2) (×6)	2.745(2) (×6)	2.743(2) (×6)	2.741(2) (×6)
	3.026(5) (×3)	3.033(4) (×3)	3.017(4) (×3)	3.022(4) (×3)	3.002(4) (×3)	3.000(4) (×3)
	2.491(5) (×3)	2.481(4) (×3)	2.493(4) (×3)	2.484(4) (×3)	2.497(4) (×3)	2.493(4) (×3)
a_r (Å)	5.4680	5.4670	5.4661	5.4640	5.4617	5.4582
α_r (deg)	60.59	60.57	60.54	60.51	60.46	60.42
V_r (Å^3)	117.15	117.02	116.88	116.67	116.41	116.09

Table 4. Spontaneous Magnetization and Characteristic Temperatures Obtained from Magnetization, ac Susceptibility, Transport, and Magnetotransport Measurements

x	0.00	0.03	0.06	0.09	0.12	0.15
M_S (emu/g) at 10 K	74	85	90	91	92	90
M_S^{cal} (emu/g)	88	88	91	92	92	90
T_M	140	170	230	280	300	320
T_c	145	175	245	290	315	330
T_R		110	200	250	275	290
T_{MR}	120 ± 10	120 ± 5	180 ± 10	230 ± 10	260 ± 10	

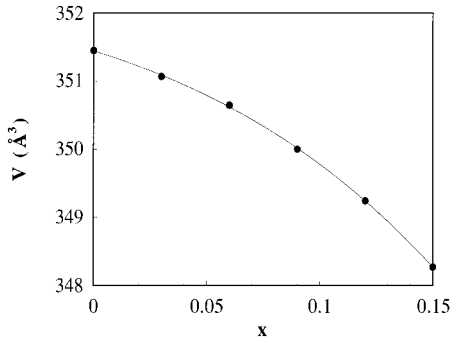

Figure 2. Hexagonal cell volume vs composition for $La_{1-x}Na_xMnO_{3+\delta}$.

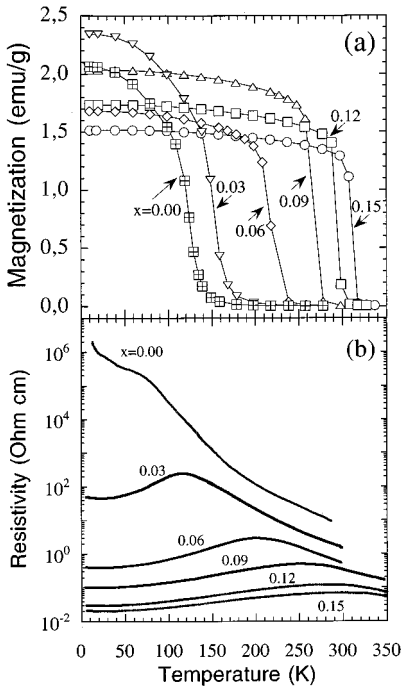

Figure 3. (a) Thermal variation of the magnetization at an applied field of 10 Oe for $La_{1-x}Na_xMnO_{3+\delta}$. (b) Thermal variation of the zero-field resistivity for $La_{1-x}Na_xMnO_{3+\delta}$.

Discussion

The use of a precursor-based synthetic method, namely, the freeze-drying of acetic solutions (ref 4 and references therein), has allowed us to synthesize single-phased perovskites at low temperatures. The formation of the perovskite phase incorporating sodium into the lattice at low-temperature avoids its evaporation at high temperatures and makes possible, in contrast to the ceramic procedure,[8] a reliable stoichiometric control. The possibility to obtain samples with controlled stoichiometry warrants appropriate discussions about tendencies in the structural and electronic properties in this series of compounds.

Unlike the ideal cubic structure, the rhombohedral structure presents an irregular 12-coordination around A cations, and a B−O−B angle that deviates substantially from 180°. Figure 2 shows the relationship between the hexagonal cell volume, *V*, and the composition in the $La_{1-x}Na_xMnO_{3+\delta}$ series. As can be observed, *V* monotonically decreases as *x* increases. This fall in the hexagonal cell volume might be considered a priori an unusual result. Indeed, as Na^+ ions are slightly larger than La^{3+} ones,[9] a certain increase of *V* with *x* might be expected, taking into account that the mean oxidation state of Mn remains nearly constant (ca. 3.33). However, a related effect was already observed in the $La_{1-x}K_xMnO_{3+\delta}$ series.[4] In this case, it might be thought that substitution of La^{3+} by the much larger K^+ cation would result in an increase in the cell volume; however, a nearly constant cell volume was observed for these compounds. Therefore, it seems reasonable to assume that there must be another factor leading to this unexpected tendencies in the cell volume with *x*.

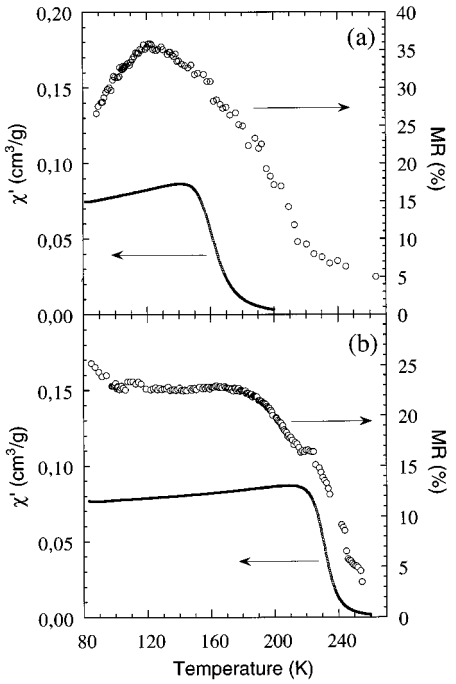

Figure 4. Thermal variation of the in-phase component of the ac susceptibility and magnetoresistance (applied field 0.9 T) for $x = 0.03$ (a) and 0.06 (b) samples.

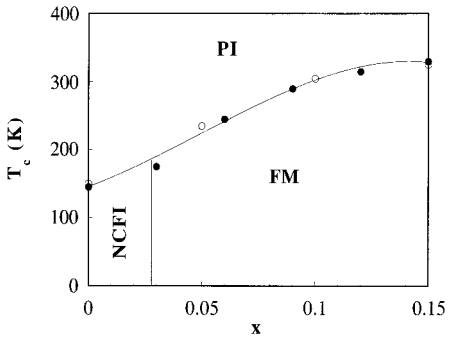

Figure 5. Electronic phase diagram of $La_{1-x}A_xMnO_{3+\delta}$, A = K, Na. (White and filled circles correspond to data for K and Na compounds, respectively).

The investigation of the thermal evolution of the structural parameters of alkaline-earth-doped manganates has shown that, upon cooling, the cell volume of these materials presents a contraction coinciding with the onset of ferromagnetic ordering.[10] This lattice contraction has been explained as the exact opposite of the lattice expansion above T_c due to the charge localization of the e_g Mn electrons, what would cause a local distortion of the lattice.[11] Thus, upon cooling, T_c is reached, e_g Mn electrons become delocalized, and the extra contribution to the cell volume vanishes. Such an interpretation would work equally to explain the volume cell variation we are dealing with. In any case, it must be taken into account that the ordering temperature, T_c, increases with x along the $La_{1-x}K_xMnO_{3+\delta}$ series. Then, although the experiments have been made at room temperature, the reduced temperature $T_r = T_{room}/T_c$, decreases with x, ranging from 2.1 for $x = 0.00$ to 0.92 for $x = 0.15$. This reduced temperature is in some way indicative of the e_g Mn electrons delocalization and, consequently, a contraction of the lattice must accompany this drop in the reduced temperature. In

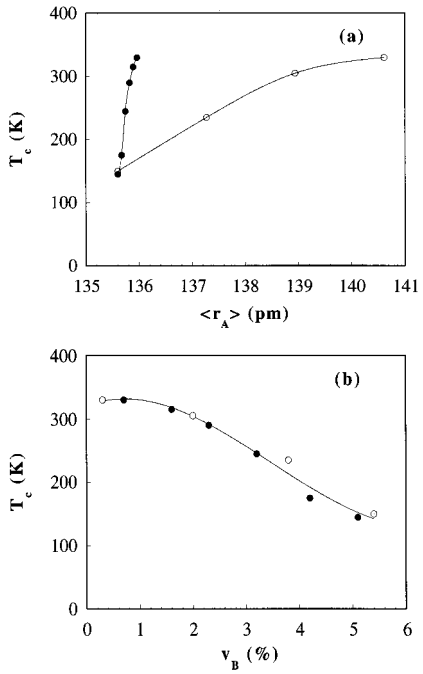

Figure 6. (a) T_c values vs mean size of cations at the B perovskite sites, $\langle r_A \rangle$, for $La_{1-x}A_xMnO_{3+\delta}$, A = K, Na. Values of $\langle r_A \rangle$ are calculated as the weighted average of crystal radii for coordination number 9 from data reported in ref 9. (b) T_c values vs concentration of vacancies at B sites, v_B, (in %) for $La_{1-x}A_xMnO_{3+\delta}$, A = K, Na. (White and filled circles, data for K and Na compounds, respectively).

the $La_{1-x}K_xMnO_{3+\delta}$ series, the expected progressive increase in the cell volume due to the substitution of the large K^+ in place of La^{3+} ions results practically compensated by the lattice contraction associated to the decreasing reduced temperature. In practice, the cell volume remains nearly constant for all the studied compositions. In contrast, in the $La_{1-x}Na_xMnO_{3+\delta}$ series, the cell expansion due to the substitution of La^{3+} by Na^+ ions ($r(Na^+) \ll r(K^+)$) is not large enough to compensate for the lattice contraction associated with the T_r drop that results in the observed lessening of the cell volume (Figure 2).

As mentioned above, we have previously found that the concentration of Mn^{4+}, c, and the mean size of cations at the A sites, $\langle r_A \rangle$, cannot fully characterize the electronic behavior of these materials.[4] In fact, this is clearly shown in Figure 6a: as can be observed, it is not possible to scale the entire T_c data set as a function of $\langle r_A \rangle$ (c is constant for all the samples). On the other hand, the representation of the electronic phase diagram (Figure 5) strongly suggests the existence of a correlation between T_c and the concentration of vacancies at the B sites, v_B [it is as well to indicate here that, for a constant Mn mean oxidation state (≈3.33), v_B is related to x and δ according to $v_B = \delta/(3 + \delta) \approx (0.165 - x)/(3.165 - x)$]. This is nicely evidenced in Figure 6b: when T_c is plotted as a function of v_B, the data referred to both potassium- and sodium-doped lanthanum manganate materials fit in well with a single curve. As can be observed, low concentrations of B vacancies have no significant effect on the electronic properties of these materials. Then, for concentrations of vacancies higher than ca. 2%, a continuous decrease in the critical temperature is observed. Notwithstanding, it seems evident that a certain variation of T_c with $\langle r_A \rangle$ could

occur for samples having the same concentration of vacancies, v_B, but in the light of the curve in Figure 6(b), this possible variation should be small compared to the effect due to the own v_B values. Indeed, preliminary experiences on several materials of composition $La_{0.85}(K_{1-y}Na_y)_{0.15}MnO_{3+\delta}$ ($\delta \leq 0.02$) indicate that the T_c remains nearly constant (T_c ca. 330 K), regardless of the y value.

Once it is established that the concentration of vacancies at the B sites plays a key role in determining the electronic properties of the lanthanide mixed-valence manganates, it seems reasonable to argue about the reasons for this influence. In a famous publication, De Gennes studied the effect of double exchange in a Bravais lattice of magnetic ions that consists of ferromagnetic layers (exchange integral $J' > 0$, transfer integral in the layer b′, z' neighboring spins) antiferromagnetically coupled (exchange integral $J < 0$, transfer integral between layers b, z neighboring spins).[12] This is in fact the situation in the undoped $LaMnO_3$ compound. The cooperative Jahn Teller ordering leads to an *ab* antiferrodistortive disposition of elongated octahedra that gives ferromagnetic exchange interactions between Mn ions in the *ab* planes and antiferromagnetic interactions between Mn ions of different planes. This A type antiferromagnetic order is modified by the cooperative rotation of the MnO_6 octahedra, which introduces an antisymmetric exchange coupling resulting in a canted spin structure.[13] De Gennes did not consider this antisymmetric exchange and predicted an antiferromagnetic ground state for doped manganates with low concentrations of Mn^{4+}. However, his predictions leading to the variation of the ordering temperature along with the doping level were in rather good agreement with subsequent experimental observations.[14]

According to De Gennes, the critical temperature for the paramagnetic to ferromagnetic transition can be expressed as the sum of two terms, namely exchange and double exchange. The exchange integrals contribute to the exchange term, whereas the transfer integrals contribute to the double exchange term

$$T_c = T_E + T_{DE}$$

$$T_E = 2kS^2/3\ (zJ + z'J')$$

$$T_{DE} = 4kx/15\ (zb + z'b')$$

where x is the hole concentration.

In the case of $La_{1-x}A_xMnO_{3+\delta}$ we are studying, the presence of B cationic vacancies can clearly affect both terms. Thus, in that concerning the double exchange interactions, the presence of cationic vacancies will perturb the periodic potential seen by the electrons, and the mobile holes will tend to become trapped at Mn sites adjacent to the vacancies.[13] The B sublattice sites could be then described as composed by (a) clusters formed by the vacancies and those neighboring Mn cations in which holes are trapped and (b) a matrix, formed by the remaining Mn cations, in which the carriers are moving. Experimental evidence that might be related with such a description is the observation of magnetic clusters (around 20 Å) in the case of $LaMnO_{3+\delta}$ samples having a high concentration of vacancies.[16] In this last case, the magnetic clusters are observed below T_c coexisting with a long-range ferromagnetic order. Actually, the formation of such magnetic clusters in $LaMnO_{3+\delta}$ samples would provide an explanation of the anomalous reduction of the observed spontaneous magnetization that, as stated above, cannot only be explained by invoking the canting effect. Under these considerations, increasing concentrations of B cationic vacancies would result in subsequent decreases of both the number of Mn ions participating in the delocalization of carriers and the number of free holes in the matrix. Consequently, the double exchange contribution to the critical temperature will diminish as v_B increase.

On the other hand, for a given manganese ion, the effective number of other immediate neighboring Mn ions will be smaller the higher the v_B is. Therefore, the exchange term contribution will vary with v_B in the same sense as the double exchange term.

In any case, given the relatively low absolute values of the vacancies' concentration, it is reasonable to assume that the main contribution to the T_c values variation results from the double exchange term, and consequently, the whole phenomenon must be driven by hole trapping.

It must be pointed out that all the above considerations have significance just because the concentration of Mn^{4+} in all the studied samples in the series $La_{1-x}A_xMnO_{3+\delta}$ (A = K, Na) remains practically constant (≈33%). If this is not so, the phenomenology is somewhat more complicated, and results from different works may appear as discordant. This is in practice the case for the studies on the effect of the oxygen content in a series of samples of stoichiometry $LaMnO_{3+\delta}$.[15−17] As far as both the concentration of vacancies in B positions (trapping centers for holes) and the concentration of Mn^{4+} (total concentration of holes) increase with δ, the electronic properties (determined by the concentration of free holes) become affected simultaneously by these two counterweighting effects, which makes comparative descriptions unrealistic.

In summary, the determination of relevant points in the electronic phase diagram of alkali-metal-doped lanthanum manganate systems with fixed concentration of Mn^{4+} has allowed us to show how the electronic properties of mixed-valence manganates with a similar concentration of holes are controlled by the concentra-

(14) Jirák, Z.; Hejtmánek, J.; Pollert, E.; Marysko, M.; Dlouhá, M.; Vratislav, S. *J. Appl. Phys.* **1997**, *81*, 5790.

(15) (a) Töpfer, J.; Goodenough, J. B. *J. Solid State Chem.* **1997**, *130*, 117. (b) Töpfer, J.; Goodenough, J. B. *Chem. Mater.* **1997**, *9*, 1467.

(16) Ritter, C.; Ibarra, M. R.; De Teresa, J. M.; Algarabel, P. A.; Marquina, C.; Blasco, J.; García, J.; Oseroff, S.; Cheong, S.-W, *Phys. Rev. B*, **1997**, *56*, 8902.

(17) (a) Töpfer, J.; Doumerc, J. P.; Grenier, J. C., *J. Mater. Res.* **1996**, *6*, 1511. (b) Ferris, V.; Brohan, L.; Ganne, M.; Tournoux, M. *Eur. J. Solid State Inorg. Chem.* **1995**, *32*, 131. (c) Ferris, V.; Goglio, G.; Brohan, L.; Joubert, O.; Molinié, P.; Dordor, P.; Ganne, M. *Mater. Res. Bull.* **1997**, *32*, 763. (d) Goglio, G.; Maignan, A.; Ferris, V.; Brohan, L.; Ganne, M. 12th International Conference on Solid Compounds of Transition Metals, Proceedings, St-Malo 22−25, 1997. (e) Arulraj, A.; Mahesh, R.; Subbanna, G. N.; Mahendiran, R.; Raychaudhuri, A. K.; Rao, C. N. R. *J. Solid State Chem.* **1996**, *127*, 87. (f) Gupta, A.; McGuire, T. R.; Duncombe, P. R.; Rupp, M.; Sun, J. Z.; Gallagher, W. J.; Xiao, G. *Appl. Phys. Lett.* **1995**, *67*, 3494. (g) Alonso, J. A.; Martinez-Lope, M. J.; Casais, M. T.; MacManus-Driscoll, J. L.; de Silva, P. S. I. P. N., Cohen, L. F.; Fernandez-Diaz, M. T. *J. Mater. Chem.* **1997**, *7*, 2139.

tion of vacancies in B positions, which can be chemically controlled by the appropiate substitution of alkaline cations in place of La^{3+} cations. These vacancies act as trapping centers for holes and, thus, a decrease in this number of vacancies by solely 5% gives rise essentially to an increase in the concentration of mobile carriers. This in turn affects the double exchange mechanism mainly and, hence, accounts for the experimentally observed enhancement with La substitution in the critical temperature.

Acknowledgment. The research in Valencia was supported by the Spanish Comision Interministerial de Ciencia y Tecnología (CICYT, MAT93-0240, MAT96-1037) and the Generalitat Valenciana (GV-1126/93, GV-2227/94). Work in Pamplona (Navarra) was supported by CICYT under the project MAT94-0964 and by the Gobierno de Navarra. The research in Sweden was supported by the Funding Agency NUTEK. Z. E.-F. is grateful to the Instituto de Cooperación con el Mundo Arabe for a grant. The SCSIE of the Universitat de València is acknowledged for X-ray diffraction and analytical facilities. It is our pleasure to acknowledge invaluable discussions with Professors V. Madurga and D. Beltrán.

CM970749H